
The Minorca Basin: a buffer zone between the Valencia and Liguro-Provençal Basins (NW Mediterranean Sea)

Pellen Romain^{1,2,*}, Aslanian Daniel¹, Rabineau Marina², Leroux Estelle³, Gorini Christian³, Silenziario Carmine⁴, Blanpied Christian⁵, Rubino Jean-Loup⁵

¹ IFREMER, Ctr Brest, GM, BP 70, F-29280 Plouzane, France.

² IUEM UBO, UMR6538, CNRS, Domaines Ocean, F-29280 Plouzane, France.

³ Univ Paris 06, UPMC, UMR 7193, ISTEP, F-75005 Paris, France.

⁴ Schlumberger House, Gatwick Airport, W Sussex, England.

⁵ CSTJF, TOTAL, TG ISS, Ave Laribeau, F-64018 Pau, France.

* Corresponding author : Romain Pellen, email address : romain.pellen@ifremer.fr

Abstract :

Detailed analyses of seismic profiles and boreholes in the Valencia Basin (VB) reveal a differentiated basin, the Minorca Basin (MB), lying between the old Mesozoic Valencia Basin sensu stricto (VBs) and the young Oligocene Liguro-Provençal Basin (LPB). The relationship between these basins is shown through the correlation of four Miocene-to-present-day megasequences. The Central and North Balearic Fracture Zones (CFZ and NBFZ) that border the MB represent two morphological and geodynamical thresholds that created an accommodation in steps between the three domains. Little to no horizontal Neogene movements are found for the Ibiza and Majorca Islands. In contrast, the counterclockwise movement of the Corso-Sardinian blocks induced a counterclockwise movement of the Minorca block towards the SE along the CFZ and NBFZ, during the exhumation of lower continental crust in the LPB. This new understanding implies pure Neogene vertical subsidence in the VBs and places the AlKaPeCa northeastward of the present-day Alboran Area.

13

14 **General Setting**

15 Although the Valencia Basin (VB) is recognized as a former Mesozoic basin
16 (Maillard, 1992; Roca, 1992, 2001; Ayala *et al.*, 2015), it is generally considered to be an
17 aborted Miocene back-arc basin in the southwestward continuation of the Liguro-Provençal
18 Basin (LPB). Two main types of models are normally proposed for its evolution during the
19 Neogene: 1) a continuity from the LPB to the Alboran domain going through the VB (e.g.
20 Doglioni *et al.*, 1997, 1999; Lonergan & White, 1997; Gueguen *et al.*, 1998; Faccenna *et al.*,
21 2004; Jolivet *et al.*, 2006) or 2) a segmented and multi-phased response between the LPB and
22 VB (e.g. Rehault *et al.*, 1984; Sanz de Galdeano 1990; Maillard & Mauffret, 1999; Maerten &
23 Seranne 1995; Roca, 2001). In both cases, the North Balearic Fracture Zone (NBFZ) played a
24 key role in this opening “swinging door” movement (as described by Martin, 2006), leading
25 to the counterclockwise rotation of the Corsica-Sardinia microplate and a clockwise rotation
26 of the Balearic promontory during the Oligocene-Early Miocene (e.g. Auzende *et al.*, 1973;
27 Dewey *et al.*, 1973; Mauffret *et al.*, 1995; Olivet, 1996; Maillard & Mauffret, 1999; Gueguen
28 *et al.*, 1998; Gattacceca *et al.*, 2007; Carminati *et al.*, 2012). Southwest of the NBFZ, two
29 secondary transfer zones are also suggested, the Central Fracture Zone (CFZ) between
30 Minorca-Mallorca islands, and the Ibiza Fracture Zone (IFZ) between Mallorca-Ibiza islands.
31 The initial rifting phase during the Neogene (Chattian / Early Burdigalian) is recorded in the
32 sedimentary strata of the Gulf of Lion (GOL) (Edel, 1980; Gorini *et al.*, 1993; Ferrandini *et*
33 *al.*, 2003; Gattacceca *et al.*, 2007) and similar deltaic to shallow marine environments are
34 recorded on the Catalan margin in the northwestern part of the VB (Roca *et al.*, 1999; Roca,
35 2001). On the Ebro margin (Tarragona trough) and on land (Valles-Penedes graben), the
36 synrift deposits are described as Burdigalian to Langhian/Early Serravallian (Clavell &

37 [Berastegui, 1991](#); [Bartrina et al. 1992](#); [Alvarez de Buergo & Melendez-Hevia 1994](#); [Cabrera](#)
38 [and Calvet, 1996](#); [Martinez Del Olmo, 1996](#); [Rodriguez-Murillas et al., 2013](#)).

39 In this study, based on a large set of seismic data and boreholes, we detail the
40 sedimentary architecture, the nature of the base of the Tertiary series, the segmentation of the
41 VB, and also highlight the role of tectonic heritage in the subsidence history of each segment.

42 **Correlation along the study area**

43 Our study is based on a large set of seismic and borehole data gathered during the extensive
44 French academia-industry programs (Actions-Marges, GRI Téthys Sud), in close
45 collaboration with the Total and Schlumberger groups (Figure 1). Due to this dense set of
46 profiles, seismic reflectors were identified and successfully correlated to previous detailed
47 studies in the LPB ([Rabineau, 2001](#); [Bache, 2008](#); [Leroux, 2012](#)). Ages of paleomarkers were
48 defined using biostratigraphic data from thirty-eight boreholes in the VB and seven boreholes
49 in the GOL.

50 The evolution and appearance of these seismic markers highlights the subdivision of
51 the area into three domains: (1) the Valencia Basin *sensu stricto* (VBss), limited to the NE by
52 the CFZ, (2) the Minorca Basin (MB) bounded by the CFZ and the NBFZ, and (3) the LPB.
53 Four megasequences are described along the VB and LPB (Figure 2):

54 (1) The Late Oligocene to Early Miocene megasequence, not visible on Figure 2, is
55 essentially limited to the Catalan and GOL graben (e.g. [Roca, 2001](#)).

56 (2) The Miocene megasequence defined in the basin lies between the Tertiary
57 basement and M30 (Figure 2). Several reflectors were correlated through the VB
58 and LPB. M03 is a high-amplitude, continuous reflector dated to the top of the
59 Burdigalian from correlation to Catalan margin boreholes (e.g. Barcelona Marino

60 B1 and C1). Its extent is limited to the MB and LPB. M06 and M08 are
61 respectively estimated to be Langhian and Latest Serravallian to Early Tortonian
62 (Benicarlo C1 and Tarragona trough boreholes). In the VBss, sediments below
63 M06 include distal and pelagic Late Burdigalian to Langhian deposits. The
64 continuity of M08 toward the MB and LPB is clearly conceivable, but a direct
65 correlation was impossible due to unfavorable morphologies. The M11, dated as
66 Late Tortonian to Early Messinian (borehole Benicarlo C1), is mainly an erosive
67 surface in the VBss, which evolves into a conformable surface in the MB (M20b).

68 (3) The Messinian megasequence comprises the Lower Unit, Mobile Unit, Upper Unit
69 (e.g. Lofi et al., 2011; Gorini et al., 2015), comprised between M30 and M30
70 surfaces. In the VBss, the base of the Upper Unit corresponds to the M30 surface,
71 which is erosive or conformable and can be correlated in the upper margin with the
72 Messinian Margin erosional surface (MES).

73 (4) The Pliocene to Quaternary megasequence covers most of the major structural
74 highs. Large prograding and pro-aggrading clinoforms characterize the shelf due to
75 high sediment supply and glacio-eustatic variations (e.g. Lofi et al., 2003;
76 Kertznus and Kneller, 2009). Two prominent surfaces, P60 and P50, were
77 correlated to Q10 and P11, dated at 0.9 Ma and 2.6 Ma, respectively (e.g.
78 Rabineau et al., 2014; Leroux et al., 2014).

79 **Segmentation and Individualization of the Minorca basin**

80 Figures 3A, 3B, 4A, and 4B emphasize the evolution of these seismic markers along 6
81 NE-SW and 3 NW-SE profiles crossing the three basins. The Oligocene-Aquitian
82 megasequence is restricted to the GOL and Catalan margins. The Miocene and Messinian
83 megasequences show a gradual thickening from the VBss towards the LPB. The thickness of

84 the Miocene megasequence increases from 0-0.9 second two-way time (stwt) (VBss) to 1.1+/-
85 0.3 stwt (MB), and is fully developed in the LPB (1.4+/- 0.4 stwt) (Figure 3B). A new seismic-
86 stratigraphic unit is also identified in the MB (green unit in Figure 3B), which increases in
87 thickness towards the LPB. Continuous reflectors with medium-amplitude clinoforms that
88 prograde toward the NE characterize this unit (Figures 2, 3B). The base of this Upper
89 Miocene prograding sequence changes rapidly, from a truncation surface (VBss) to a
90 correlative conformity (MB), and shows an increase in depth, from 3.3 s (VBss) to 4.5 s
91 (MB), and ultimately to 5.2 s (LPB). The thickness of the Messinian megasequence varies:
92 0.05 to 0.3 s in the VBss, 0.6 to 0.7 s in the MB, and > 1.26 s in the LPB. Furthermore, the
93 MB is characterized by the development of the Lower Unit and Mobile Unit (in the NE),
94 whereas the full development of the Lower and Mobile units is limited to the LPB. The base
95 of the Mobile Unit also evolves, from 4.5 s in the MB to ~5 s in the LPB. For Pliocene and
96 Quaternary deposits, the variation in thickness is mainly controlled by sedimentary transport
97 from the Ebro river (Nelson, 1990) and the Rhône river for the deep LPB (e.g. Leroux, 2012).

98 The segmentation into three domains appears in the Bouguer anomaly map and the
99 residual geoid anomaly map, which show a strong SW-NE segmentation between the LPB,
100 MB, and VBss (Ayala *et al.*, 2015), and also on the base of Tertiary map of the entire VBss-
101 MB-LPB area (Figure 5). The base of the Tertiary in the MB presents a mean depth of 4.6 +/-
102 0.5 (stwt), intermediate between the VBss (3.5 +/- 0.3 stwt) and the deeper LPB (6.5 +/- 0.2
103 stwt) (Figure 3B). This segmentation is clearly depicted by the CFZ to the southwest of the
104 MB and by the NBFZ to the northeast of the MB (Maillard & Mauffret, 1999). These
105 differences in depth imply a difference in Neogene subsidence in the three segments,
106 decreasing towards the SW. This is also observed in the first occurrences of marine
107 sediments, which started at the Oligocene in the LPB and the Catalan margin (MB), and only

108 at the Late Burdigalian-Langhian in the VBss (Figure 6). The Neogene subsidence in the
109 VBss started later than it did in the LPB and MB.

110 Alternatively, some authors suggest another segment in the VBss with the Ibiza
111 Fracture Zone (IFZ) (Maillard & Mauffret, 1999) explaining the suggested clockwise 93 km
112 southeastward movement of Mallorca block. However, the authors state that IFZ is “*not*
113 *documented as there is no or very little information in that region*”, its presence was only
114 presumed due to differences in crustal thicknesses (suggested to reach 13 km in the
115 southwestern part). However, modern high-quality data presented by Alaya *et al.* (2015)
116 falsifies this view and shows instead a thickness of 5 to 6 km in the SW part. Previous studies
117 identified a Mesozoic basin in the whole VBss (e.g. Roca, 1992; Maillard, 1993), with a
118 maximum thickness reaching more than 3 km. Toward the Balearic promontory the Estudio
119 Sismico de la Corteza Ibérica (ESCI) profiles show a continuation of this Mesozoic basin
120 (Roca *et al.*, in Cavazza *et al.*, 2004) and we infer that the VBss extends between the Ibiza
121 and Mallorca Islands and the Ebro-Tarragona margin. In contrast, in the MB and LPB, the
122 substratum is characterized by chaotic, hyperbolic, and medium-amplitude reflectors (Figures
123 2b and 2c). In the MB, mean velocities from the ESP60 profile (Figure 3B, cross section 3)
124 were 4.2 to 6.1 km/s in the upper part of the Tertiary basement and were interpreted as
125 Neogene volcanic layers (Mauffret *et al.*, 1995) (Figures 2, 3B, 4B). In the LPB, the domain
126 limited between hinge line 3 and the proto-oceanic crust limit (Figure 5) has recently been
127 identified as a thin layer of lower continental crust (C.C.) (Moulin *et al.*, 2015), exhumed
128 along a landward deep detachment (Séranne, 1999) and overlying an heterogeneous, intruded
129 layer (gabbros or granulites), with velocities of 6.0 and 6.4 km/s for the upper layer and 6.6 to
130 7.5 km/s for the lower layer (Moulin *et al.*, 2015).

131 **The Minorca Basin, a buffer segment**

132 As previously shown by Roca (1992) and Ayala *et al.* (2015), there is little to no
133 evidence of Neogene horizontal movement (no extension, very few faults observable on
134 seismic data) in the offshore Mesozoic sedimentary sequences of the VBss. The neogene syn-
135 rift deposits are localized either on land or on the MB borders (Figure 4, zoom A).
136 Paleomagnetic data on the Balearic Islands describes two phases of Miocene rotation and is
137 usually used for geodynamic reconstruction. However, these two phases of rotation are linked
138 to the Betics compressive phase and should not be connected with the kinematic rotation of
139 the islands (Parès *et al.*, 1992). If a rift had propagated into the VBss, the Mesozoic
140 sedimentary sequences should also have been affected by the extension. On the contrary, the
141 Neogene sedimentary layers in the central part of the VBss are horizontal and parallel (Figure
142 4, zooms B and C), which implies a vertical subsidence during this period, as has been
143 described in sag basins where no extensive movements are depicted (Moulin *et al.*, 2005;
144 Aslanian *et al.*, 2009). The significant thickness of Mesozoic deposits associated with
145 thinning of the crust have led Roca and Guimera (1992) to propose a Mesozoic thinning that
146 would account for at least half of the entire thinning, implying a huge tectonic heritage in the
147 VBss. It is beyond the scope of this paper to discuss the genesis of the Mesozoic basin, but for
148 the Neogene phase, movement of the Ibiza-Mallorca blocks toward the southeast in the VBss
149 would imply major extensive deformations in the Mesozoic deposits, which are not observed
150 on seismic data (Roca, 1992; Ayala *et al.*, 2015).

151 Following what was suggested by previous authors (e.g. Tassone *et al.*, 1996; Roca *et*
152 *al.*, 1999), our results show that the MB and LPB exhibit the same Oligo-Miocene
153 synchronous syn-rift sedimentary sequence, which does not support the hypothesis of rift
154 propagation that should have produced diachronous sequences. The continuity between the
155 two basins is further substantiated by the first occurrences of marine sediment at Oligocene
156 times in the LPB and the Catalan margin (MB) (Figure 6).

157 The position of the almost rigid Corso-Sardinian block (Arthaud and Matte, 1977)
158 before the Miocene rift phase implies that the Minorca block was about 100 km closer to the
159 Catalan margin (Figures 6 and 8) at that time (e.g. Le Cann, 1987; Olivet, 1996). The NBFZ,
160 which was, during the Pyrenean compressive phase, a dextral N-S transfer zone between the
161 Iberian and Corso-Sardinian microplates (e.g. Olivet, 1996), was reactivated during the Oligo-
162 Miocene extension phase, leading to the counterclockwise movement of the Corso-Sardinian
163 block, which is accompanied by the counterclockwise movement of the Minorca block to the
164 SE along the CFZ (Le Cann, 1987; Gueguen, 1995; Olivet, 1996), contrary to what was
165 proposed based on scarce paleomagnetic data on the Balearic Island (Parès *et al.*, 1992). This
166 movement coincides with the exhumation of the 4 km-thick lower C.C. in the LPB (a
167 metamorphic core complex for Jolivet *et al.*, 2015). This movement stopped when the proto-
168 oceanic crust started (Moulin *et al.*, 2015). During the Early Miocene-Messinian times, the
169 two transfer zones, CFZ and NBFZ, accommodate the subsidence between the VBss (high
170 position) and the LPB (deep domain) (Figures 3A, 3B).

171 While both VBss and LPB segments, (Leroux *et al.*, 2015), exhibit pure vertical subsidence
172 (Figures 4B), the thinning process may not be the same, as VBss is a polyphased basin, and
173 the LPB thinning was only during the Neogene and due to the exhumation of the lower C.C..
174 In between the VBss and LPB, the Minorca Neogene movement may have involved an
175 exhumation, such as in the GOL, but the substratum may also comprise stretched and intruded
176 upper C.C.. This issue is still open and will need the acquisition of additional wide-angle
177 seismic data in the MB to be able to address the uncertainties.

178 The idea that the MB should be considered as a Neogene buffer zone between the young
179 Oligocene-to-Miocene LPB and the old Mesozoic VBss, modifies the general view of the
180 northern part of the Occidental Mediterranean Sea before opening (Figure 7). First, the
181 divergent movements of the Kabylia blocks on one side and Peloritain-Calabria blocks on

182 the other side appear at the southwards end of the buffer zone. Second, little to no Neogene
183 movements for the Ibiza and Majorca Islands place the AlKaPeCa group (Alboran, Kabyle,
184 Peloritain, and Calabrian blocks; e.g. [Mauffret *et al.*, 1995](#)) further to the southeast,
185 northeastward of what is at present-day the Alboran Area.

186

187 **ACKNOWLEDGEMENTS**

188 This work was supported by the "Laboratoire d'Excellence" LabexMER (ANR-10-LABX-19)
189 and co-funded by a grant from the French government under the program "Investissements
190 d'Avenir", and by a grant from the Regional Council of Brittany.

191 It was further supported by CNRS and IFREMER, with additional support from the French
192 Actions-Marges program (J.L. Rubino & P. Unternehr) and the GRI Méditerranée
193 (Groupement Recherche et Industrie TOTAL-UPMC). The database was built thanks to the
194 SIGEOF spanish site and cruises from French and Spanish teams. Additional industrial
195 seismic lines were provided by Schlumberger. The authors acknowledge the fruitful and
196 constructive reviews by Alexander Keith Martin and Francesca Sabat, as well as those from
197 the editor Carlo Doglioni and his associate editor that greatly improved the manuscript.

198 **Competing financial interests**

199 The authors declare no competing financial interests.

200 REFERENCES

- 201 Afilhado A., Moulin M., Aslanian D., Schnürle P., Klingerhoefer F., Nouzse H., Rabineau M.,
202 Leroux E. and Beslier M.-O., 2015. Deep crustal structure across a young passive
203 margin from wide-angle and reflection seismic data (The SARDINIA Experiment) – II.
204 Sardinia's margin. *Bulletin de la Société géologique de France*, **186** (4-5), 331-351.
- 205 Alvarez de Buergo E., Meléndez-Hevia F., 1994. Características generales de las subcuencas
206 del margen peninsular mediterráneo (“Rift” del Surco de Valencia). *Acta geologica*
207 *Hispanica*, **29** (1), 67-79.
- 208 Araña V., Aparicio A., Martin-Escorza C., Garcia-Cacho L., Ortiz R., Vaquer R., Barbieri F.,
209 Ferrara G., Albert J. and Gassiot X., 1983. El volcanismo neogeno-cuaternario de
210 Catalunya : caracteres estructurales, petrologicos y geodinamicos. *Acta geologica*
211 *Hispanica*, **18** (1), 1-17.
- 212 Arthaud F. and Matte P., 1977. Détermination de la position initiale de la Corse et de la
213 Sardaigne à la fin de l'orogénèse hercynienne grâce aux marqueurs géologiques
214 antémésozoïques. *Bulletin de la Société Géologique de France*, **7**, 833-840.
- 215 Aslanian D., Moulin M., Olivet J.-L., Unternehr P., Matias L., Bache F., Rabineau M., Nouzé
216 H., Klingelhoefer F., Contrucci I., Labails C., 2009. Brazilian and African passive
217 margins of the Central Segment of the South Atlantic Ocean/ Kinematic constraints.
218 *Tectonophysics*, **468**, 98-112.
- 219 Auzende J.M., Bonnin J. and Olivet J.L., 1973. The origin of the Western Mediterranean
220 basin. *Journal of the Geological Society of London*, **19**, 607–620.
- 221 Ayala, C., Torne M. and Pous J., 2003. The lithosphere asthenosphere boundary in the
222 western Mediterranean from 3D joint gravity and geoid modeling: tectonic implications.
223 *Earth Planetary Science Letters*, **209**, 275-290.

224 Ayala C., Torne M. and Roca E., 2015. A review of the current knowledge of the crustal and
225 lithospheric structure of the Valencia Trough Basin, *Boletín Geológico y Minero*, **126**
226 (2-3); 533-552.

227 Bache F., 2008. Evolution Oligo-Miocène des marges du micro océan Liguro-Provençal.
228 Thèse de doctorat de l'université de Bretagne Occidentale, Brest. 328 pp.

229 Bache, F., Olivet, J.L., Gorini, C., Aslanian, D., Labails, C. and Rabineau, M., 2010.
230 Evolution of rifted continental margins: the cases of the Gulf of Lion (western
231 Mediterranean basin). *Earth and Planetary Science Letters*, **292** (3-4), 345-356, 2010.

232 Bartrina M.T., Cabrera L., Jurado M.J., Guimerà J. and Roca E., 1992. Evolution of the
233 Central Catalan margin of the Valencia trough (western Mediterranean).
234 *Tectonophysics*, **203**, 219-247.

235 Cabrera, L. and Calvet, F., 1996. Onshore Neogene record in NE Spain: Vallès-Penedès and
236 El camp half-grabens (NW Mediterranean). In: *Tertiary Basins of Spain the*
237 *Stratigraphic Record of Crustal Kinematics: World and Regional Geology* (P.F. Friend
238 and C.J. Dabrio eds). Cambridge University Press, Cambridge.

239 Carminati E., Lustrino M. and Doglioni C., 2012. Geodynamic evolution of the central and
240 western Mediterranean: Tectonics vs. igneous petrology constraints. *Tectonophysics*,
241 **579**, 173-192.

242 Cavazza, W., Roure, F., Spakman, W., Stampfli, G.M. and Ziegler, A., 2004. *The*
243 *TRANSMED Atlas, the Mediterranean Region From Crust to Mantle*.
244 Springer, Berlin, 141 pp.

245 Clavell E. and Berastegui X., 1991. Petroleum geology of the Gulf of València. *Generation,*
246 *accumulation, and production of Europe's hydrocarbons* (Ed. A.M. Spencer), *Special*
247 *Publication of the European Association of Petroleum Geoscientists*, **1**, 355-368.

- 248 Dewey, J.F., Pittman, W.C., Ryan, W.B.F. and Bonin, J., 1973. Plate tectonics and the
249 evolution of the Alpine system. *Geol. Soc. Am. Bull.*, **84**, 3137-3180.
- 250 Doglioni C., Gueguen E., Sàbat F., Fernandez M., 1997. The Western Mediterranean
251 extensional basins and the Alpine orogeny. *Terra Nova*, **9**, 109-112.
- 252 Doglioni C., Fernandez M., Gueguen E., Sàbat F., 1999. On the interference between the early
253 Apennines-Maghrebides backarc extension and the Alps-Betics orogen in the Neogene
254 Geodynamics of the Western Mediterranean. *Bullotino de la Sociata Geologica Italia*,
255 **118**, 75-89.
- 256 Edel J.B., 1980. Etude paléomagnétique en Sardaigne. Conséquences pour la géodynamique
257 de la Méditerranée occidentale. Thèse de doctorat de l'Institut de Physique du Globe.
258 Université Louis Pasteur, Strasbourg, 310 pp.
- 259 Faccenna C., Piromallo, C., Crespo-Blanc A., Jolivet L., Rossetti F., 2004. Lateral slab
260 deformation and the origin of the western Mediterranean arcs. *Tectonics*, **23**, TC1012.
- 261 Ferrandini, J., Gattacceca, J., Ferrandini, M., Deino, A. and Janin, M.-C., 2003.
262 Chronostratigraphie et paléomagnétisme des dépôts oligo-miocènes de Corse:
263 implications géodynamiques pour l'ouverture du bassin liguro-provençal. *Bulletin de la*
264 *Société géologique de France*, **174**, 357-371.
- 265 Gattacceca J., Deino A., Rizzo R., Jones D.S., Henry B., Beaudoin B. and Valeboin F., 2007.
266 Miocene rotation of Sardinia: New paleomagnetic and geochronological constraints and
267 geodynamic implications. *Earth and Planetary Science Letters*, **258**, 359-377.
- 268 Gorini C., Le Marrec A. and Mauffret A., 1993. Contribution to the structural and
269 sedimentary history of the Gulf of Lions (Western Mediterranean) from the ECORS
270 profiles, industrial seismic profiles and well data. *Bulletin de la Société géologique de*
271 *France*, **164**, 353-363.

272 Gorini C., Montadert L. And Rabineau M., 2015. New imaging of the salinity crisis: Dual
273 Messinian lowstand megasequences recorded in the deep basin of both the eastern and
274 western Mediterranean. *Marine and Petroleum Geology*, **66**, 278-294.

275 Gueguen, E. 1995. Le bassin Liguro-Provençal: un véritable océan. Exemple de segmentation
276 des marges et de hiatus cinématique. Implications sur les processus d'amincissement
277 crustal. Doctorat, Université de Bretagne Occidentale, Brest, 309 pp.

278 Gueguen E., Doglioni C. and Fernandez M., 1998. On the post-25 Ma geodynamic evolution
279 of the western Mediterranean. *Tectonophysics*, **298**, 259-269.

280 Jolivet L., Augier R., Robin C., Suc J.-P. and Rouchy J.M., 2006. Lithospheric-scale
281 geodynamic context of the Messinian salinity crisis. *Sedimentary Geology*, **188-189**, 9-
282 33.

283 Jolivet L., Gorini C., Smit J. and Leroy S., 2015. Continental breakup and the dynamics of
284 rifting in back-arc basins: The Gulf of Lion margin. *Tectonics*, **34**,
285 doi:10.1002/2014TC003570.

286 Kertznus V. and Kneller B., 2009. Clinoform quantification for assessing the effects of
287 external forcing on continental margin development. *Basin Research*, **21**, 738-758. doi:
288 10.1111/j.1365-2117.2009.00411.x.

289 Le Cann C., 1987. Le diapirisme dans le bassin Liguro-Provençal (Méditerranée occidentale).
290 Relation avec la tectonique et la sédimentation. Conséquences géodynamiques. Thèse
291 de Doctorat, Université de Bretagne Occidentale, Brest.

292 Leroux E., 2012. Quantifications des flux sédimentaires et de la subsidence dans le bassin
293 Provençal, Méditerranée Occidentale. Thèse de Doctorat de l'Université de Bretagne
294 Occidentale, Brest, 455 pp.

295 Leroux E., Rabineau M., Aslanian D., Granjeon D., Gorini C. and Droz L., 2014.
296 Stratigraphic simulation on the shelf of the Gulf of Lion: testing subsidence rates and

297 sea-level curves during Pliocene and Quaternary. *Terra Nova*, **26** (3), 230-238. doi:
298 10.1111/ter.12091.

299 Leroux E., Aslanian D., Rabineau M., Moulin M., Granjeon D., Gorini C. and Droz L., 2015.
300 Sedimentary markers: a window into deep geodynamic processes, *Terra Nova*, doi:
301 10.1111/ter.12139.

302 Lofi J., Rabineau M., Gorini C., Berné S., Clauzon G., De Clarens P., Tadeu Dos Reis A.,
303 Mountain G.S., Ryan W.B.F., Steckler M.S., Fouchet C., 2003. Plio-Quaternary
304 prograding clinoform wedges of the western Gul of Lion continental margin (NW
305 MEditerranean) after the Messinian Salinity Crisis. *Marine Geology*, **198**, 289-317.

306 Lofi J., Sage F., Déverchère J., Loncke L., Maillard A., Gaullier V., Thinon I., Gillet H.,
307 Guennoc P. and Gorini C., 2011. Refining our knowledge of the Messinian salinity
308 crisis records in the offshore domain through multi-site seismic analysis. *Bulletin de la*
309 *Société géologique de France*, **182** (2), 163-180.

310 Lonergan L., White, N., 1997. Origin of the Betic-Rif mountain belt. *Tectonics*, **16** (3), 504-
311 522.

312 Maerten L. and Séranne M., 1995. Extensional tectonics of the Oligo-Miocene Hérault Basin
313 (S France), Gulf of Lion margin. *Bulletin de la Société géologique de France*, **166** (6),
314 739-749.

315 Maillard A., 1993. Structure et riftogénèse du golfe de Valence (méditerranée Nord-
316 Occidentale). Thèse de Doctorat, Université Paul Sabatier, Toulouse, 292 pp.

317 Maillard A., Mauffret A., Watts A.B., Torné M., Pascal G., Buhl P. and Pinet B., 1992.
318 Tertiary sedimentary history and structure of the Valencia trough (Western
319 Mediterranean). *Tectonophysics*, **203**, 57-75.

320 Maillard A. and Mauffret A., 1993. Structure et volcanisme de la fosse de Valence
321 (Méditerranée nord-occidentale). *Bulletin de la Société géologique de France*, **164** (3),
322 365-383.

323 Maillard A. and Mauffret A., 1999. Crustal structure and riftogenesis of the Valencia Trough
324 (north-western Mediterranean Sea). *Basin Research*, **11**, 357-379.

325 Martin A.K., 2006. Oppositely directed pairs of propagating rifts in back-arc basins: Double
326 saloon door seafloor spreading during subduction rollback. *Tectonics*, **25**, TC3008,
327 doi:10.1029/2005TC001885.

328 Martinez del Olmo W., 1996. Depositional Sequences in the Gulf of Valencia Tertiary Basin.
329 *in P.F. Friend & C.J. Dabrio (Ed.), Tertiary Basins of Spain the Stratigraphic Record*
330 *of Crustal Kinematics: World and Regional Geology, Cambridge University Press,*
331 *Cambridge, 55-67.*

332 Mauffret A., Pascal G., Maillard A. and Gorini C., 1995. Tectonics and deep structure of the
333 north-western Mediterranean Basin. *Marine and Petroleum Geology*, **12**: 645-666.

334 Meulenkamp J.E., Sissingh W., 2003. Tertiary palaeogeography and tectonostratigraphic
335 evolution of the Northern and Southern Peri-Tethys platforms and the intermediate
336 domains of the African-Eurasian convergent plate boundary zone. *Palaeogeography,*
337 *Palaeoclimatology, Palaeoecology*, **196**, 209-228.

338 Moulin M., Klingelhoefer F., Afilhado A., Aslanian D., Schnurle P., Nouzé H., Rabineau M.,
339 Beslier M.-O. and Feld A., 2015. Deep crustal structure across a young passive margin
340 from wide-angle and reflection seismic data (The SARDINIA Experiment) – I. Gulf of
341 Lion's margin. *Bulletin de la Société géologique de France*, **186** (4-5), 309-330.

342 Nelson C.H., 1990. Estimated post-Messinian sediment supply and sedimentation rates on the
343 Ebro continental margin, Spain. *Marine Geology*, **95**, 395-418.

344 Olivet, J.L., 1996. La Cinématique de la plaque Ibérique, *Bulletin des Centres de Recherches*
345 *Exploration–Production Elf Aquitaine*, Vol. 20. Pau, France, pp. 131–195.

346 Parés J.M., Roca E., Freeman R., 1992. Paleomagnetic data from the margins of the Valencia
347 trough. The role of rotations in the Neogene structuration. *Física de la Tierra*, **4**, 231-
348 246.

349 Rabineau M., 2001. Un modèle géométrique et stratigraphique des séquences de dépôts
350 Quaternaire sur la marge du Golfe du Lion : Enregistrement des cycles climatiques de
351 100 000 ans. Thèse de doctorat, Université de Rennes 1/IFREMER.

352 Rabineau M., Leroux E., Aslanian D., Bache F., Gorini C., Moulin M., Molliex S., Droz L.,
353 Reis A.D., Rubino J.-L., Guillocheau F. and Olivet J.-L., 2014. Quantifying subsidence
354 and isostatic readjustment using sedimentary paleomarkers, example from the Gulf of
355 Lion. *Earth and Planetary Science Letters*, **388**, 1-14.

356 Rehault J.P., Boillot G. and Mauffret A., 1984. The western Mediterranean Basin: geological
357 evolution. *Marine Geology*, **55**, 447-477.

358 Roca E., 1992. L'estructura de la conca Catalano-Balear: Paper de la compression I de la
359 distension en la seva gènesi. Tesi doctoral de universitat de Barcelona.

360 Roca E., 2001. The Northwest Mediterranean Basin (Valencia Trough, Gulf of Lions and
361 Liguro-Provençal basins): structure and geodynamic evolution. In; *Peri-Tethys Memoir*
362 *6: Peri-Tethyan Rift/ Wrench Basins and Passive Margins* (P.A. Ziegler, W. Cavazza,
363 A.H.F. Robertson and S. Crasquin-Soleau, eds). *Mémoire du Muséum national des*
364 *Hirtoire naturelle*, **186**, 671-706.

365 Roca E. and Guimerà J., 1992. The Neogene structure of the eastern Iberian margin: structural
366 constraints on the crustal evolution of the Valencia trough (western Mediterranean).
367 *Tectonophysics*, **203**, 203-218.

- 368 Roca E., Sans M., Cabrera L. and Marzo M., 1999. Oligocene to Middle Miocene evolution of
369 the central Catalan margin (northwestern Mediterranean). *Tectonophysics*, **315**, 209-
370 233.
- 371 Rodriguez-Morillas N., Playà E., Travé A., Martin-Martin J.D., 2013. Diagenetic processes in
372 a partially dolomitized carbonate reservoir : Casablanca oil field, Mediterranean Sea,
373 offshore Spain. *Geologica Acta*, **11** (2), 195-214.
- 374 Sanz de Galdeano C., 1990. Geologic evolution of the Betic Cordilleras in the Western
375 Mediterranean, Miocene to the present. *Tectonophysics*, **172**, 107-119.
- 376 Séranne M., Benedicto A., Labaume P., Truffet C., Pascal G., 1995. Structural style and
377 evolution of the Gulf of Lion Oligo-Miocene rifting: role of the Pyrenean orogeny.
378 *Marine and Petroleum Geology*, **12**, 809-820.
- 379 Séranne M., 1999. The Gulf of Lion continental margin (NW Mediterranean) revisited by
380 IBS: an overview. In: *The Mediterranean Basins: Tertiary Extension Within the Alpine*
381 *Orogen* (B. Durand, L. Jolivet, F. Horváth and M. Séranne, eds). *Special Publication*
382 **156**, pp. 15-36. The Geological Society, London.
- 383 Tassone E., Roca E., Muñoz J.A., Cabrera L. and Canals M., 1996. Evolucion del sector
384 septentrional del margen continental catalan durante el Cenozoico. *Acta Geologica*
385 *Hispanica*, **29** (2-4), 3-37.

386 FIGURES

387 Figure 1: Location of the study area and dataset on the bathymetric and geological map of the
388 Valencia basin s.l. Red boxes indicate location of seismic profiles presented in Figure 2,
389 showing (from SW to NE) details of the Valencia basin s.s. (VBss), the Minorca basin
390 (MB), and the Liguro-Provençal basin (LPB). Green box indicate location of seismic
391 profiles zooms presented in Figure 4.

392 Figure 2: Correlation of stratigraphic markers from the SW (VBss) to the NE (MB and LPB).
393 Names of Liguro-Provençal markers are derived from previous study (Bache, 2008;
394 Leroux, 2012). Locations of seismic profiles are shown on Figure 1.

395 Figure 3A: Non-interpreted seismic profiles oriented SW-NE (location Figure 1) crossing the
396 three defined Valencia s.s., Menorca and Ligurian-Provençal basins. MEDS76 profiles
397 were provided courtesy of Schlumberger multicient.

398 Figure 3B: Interpreted seismic profiles oriented SW-NE (location on Figures 1), highlighting
399 the evolution of the Burdigalian-Messinian, Messinian trilogy and Pliocene-Quaternary
400 megasequences and showing the general characteristics of each basin (explanation in
401 the text).

402 Figure 4A: Non-interpreted seismic profiles oriented NW-SE (location on Figure 1) illustrating
403 the Valencia s.s., Menorca and Ligurian-Provençal basins. Three zooms illustrate the
404 various structural and subsidence style between the Catalan margin (MB) (zoom 1), the
405 Tarragona trough (VBss) (zoom 2) and VBss's central depression (zoom 3). MEDS76
406 and MSP74 profiles were provided courtesy of Schlumberger multicient.

407 Figure 4B: Interpreted seismic profiles oriented NW-SE (location on Figure 1) highlighting the
408 evolution of the Oligocene-Aquitainian, Burdigalian-Messinian, and Pliocene-
409 Quaternary megasequences and showing the general characteristics of each basin. On
410 the Catalan margin the major half-graben is formed by major normal faults which led to

411 the deposition of a sedimentary wedge during Oligocene to Aquitanian (zoom 1). On the
412 contrary VBss basin records sub-parallel, horizontal and isopach strata in the deepest
413 area during Langhian to Serravallian times (zoom 2 and 3). Sediments deformation are
414 only due to triassic salt diapir activity (zoom 2).

415 Figure 5: Tertiary basement map in two-way time (s) of the NW Mediterranean sea
416 highlighting the depth increase in steps from the VBss to the LPB. Two NW-SE
417 oriented thresholds individualize the Minorca basin (CFZ: Central Fracture Zone;
418 NBFZ: North Balearic Fracture Zone). Hinge Lines highlighted in the Liguro-Provençal
419 basin show the main boundaries in the crustal evolution and subsidence response (from
420 Leroux et al., 2015; Moulin et al., 2015). Cartography of the atypical oceanic crust
421 result from a compilation of gravimetric, magnetic and velocity response (e.g. from
422 Bache, 2008; Moulin *et al.*, 2015; Afilhado *et al.*, 2015).

423 Figure 6: Paleogeographic maps of the Valencia s.l. and Liguro-Provençal domains showing a
424 repartition of marine water during Oligocene, Burdigalian and Langhian time. Circles
425 represent facies observations from boreholes. Paleocoast positions are from
426 Meulenkamp & Sissingh, 2003; Jolivet *et al.*, 2006; Roca *et al.*, 1999 combined to our
427 seismic correlations.

428 Figure 7: Northwestern Mediterranean cinematic reconstruction before opening of Liguro-
429 Provençal, Minorca and Algerian domains. Two options concerning the initial position
430 of Ibiza and Majorca are shown. In red, Early Neogene situation of Corso-Sardinian,
431 Minorca and Ibiza-Mallorca blocks proposed in this study (also suggested in Le Cann,
432 1987, Olivet, 1996, Bache, 2008, Bache *et al.*, 2010) (option a-no movement for Ibiza
433 and Mallorca islands). In purple Early Neogene situation proposed by previous studies
434 e.g. Maillard and Mauffret (1999) (option b-large movement for the Ibiza-Mallorca
435 islands). The position of AlKaPeCa blocks are from Mauffret *et al.* (1995). Two options

436 concerning the initial situation of Alboran domain are also proposed following e.g.
437 Mauffret et al. (1995) (option 1) and e.g. Doglioni et al. (1997) (option 2). The hachured
438 area corresponds to the present day exhumed lower continental crust position as
439 interpreted by Moulin *et al.* (2015).
440

Figure 1

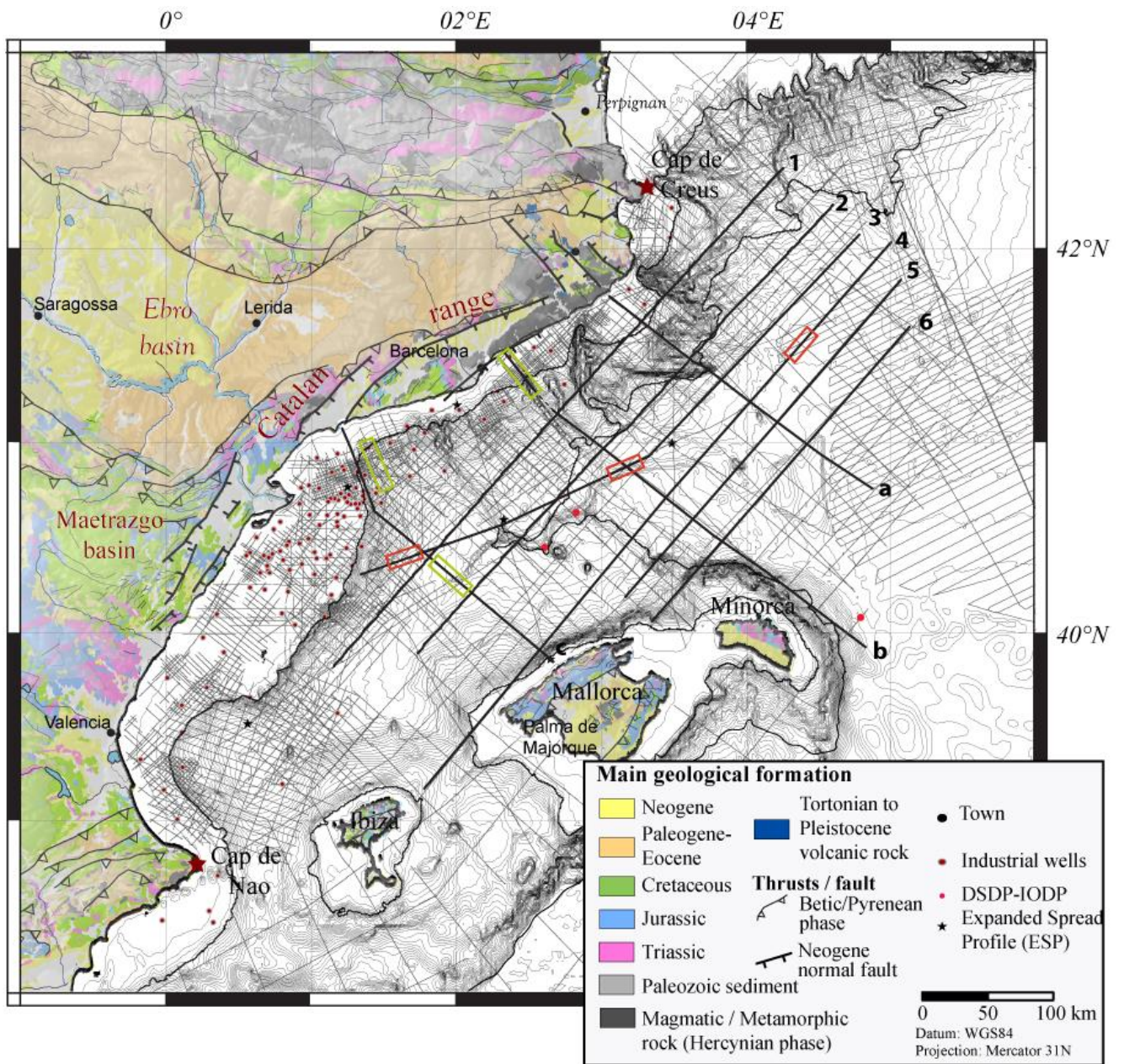
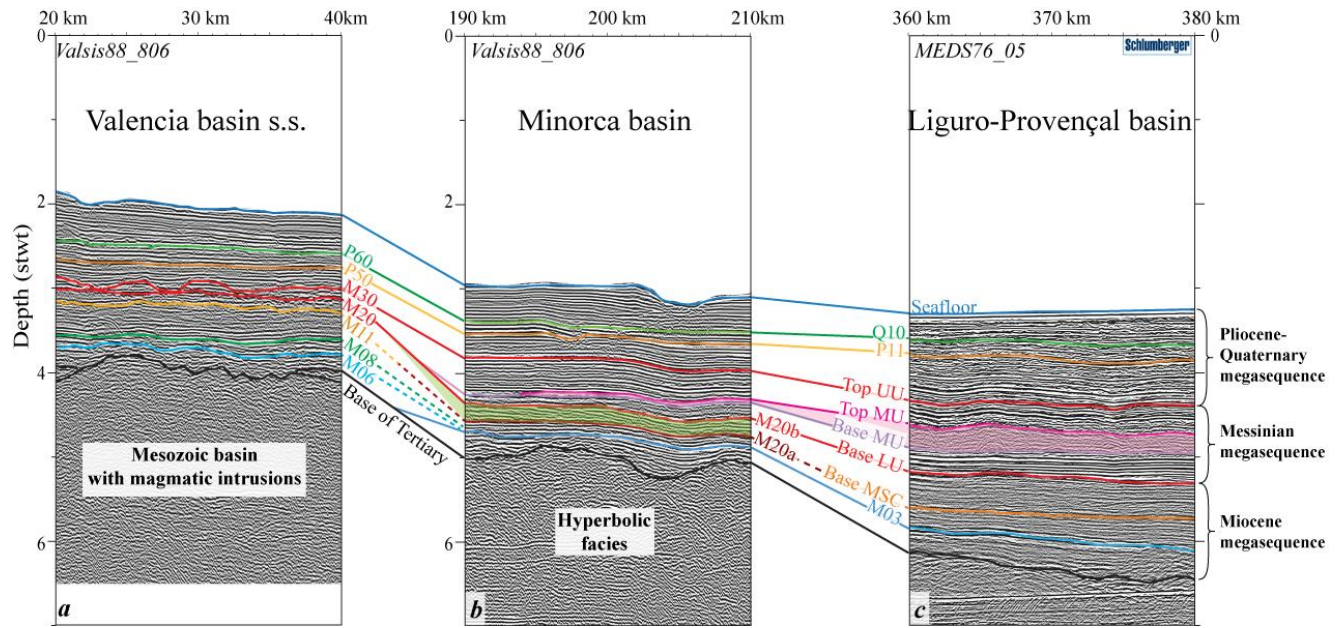


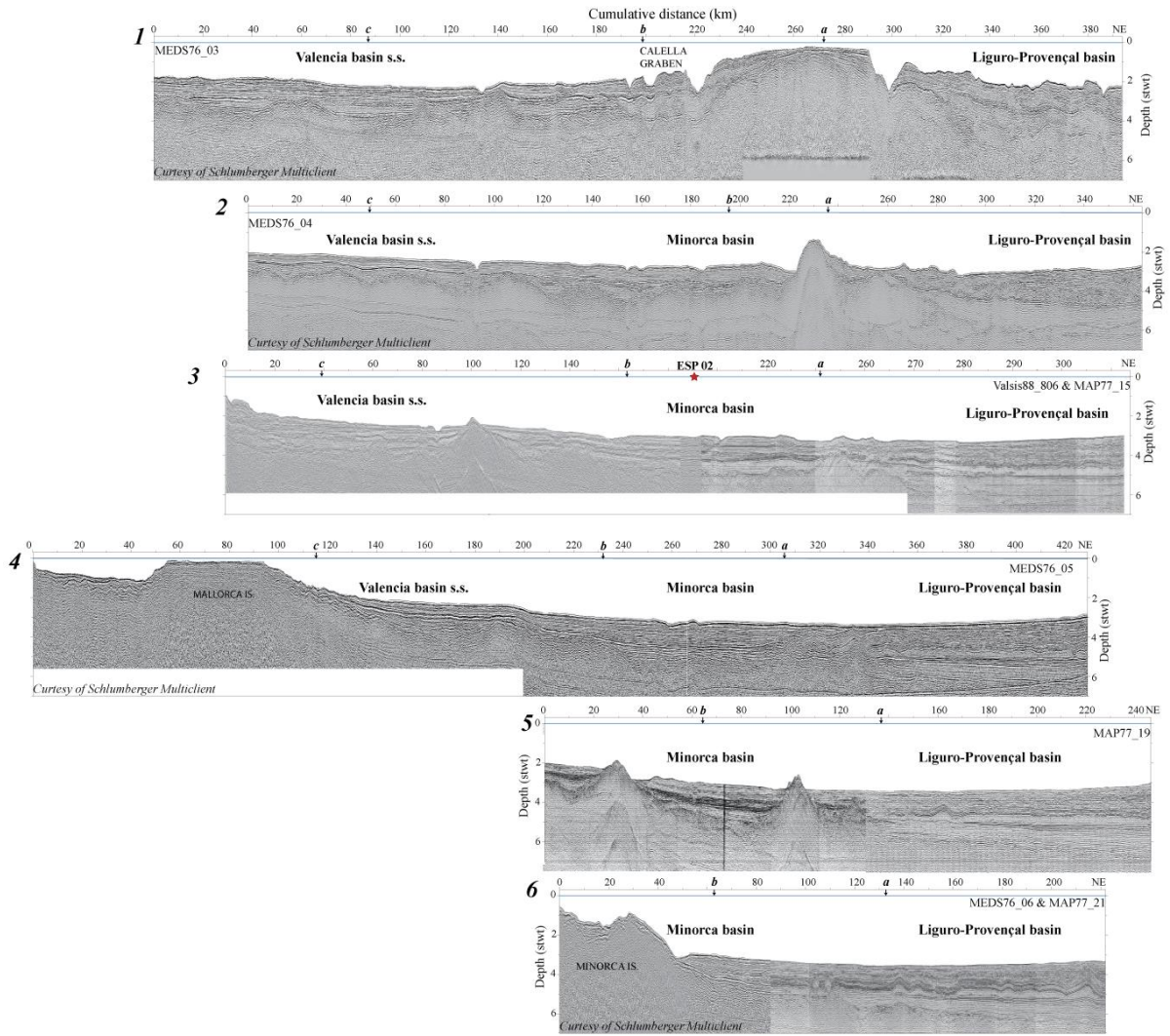
Figure 2

441



442 **Figure 3A**

443



444

Figure 3B

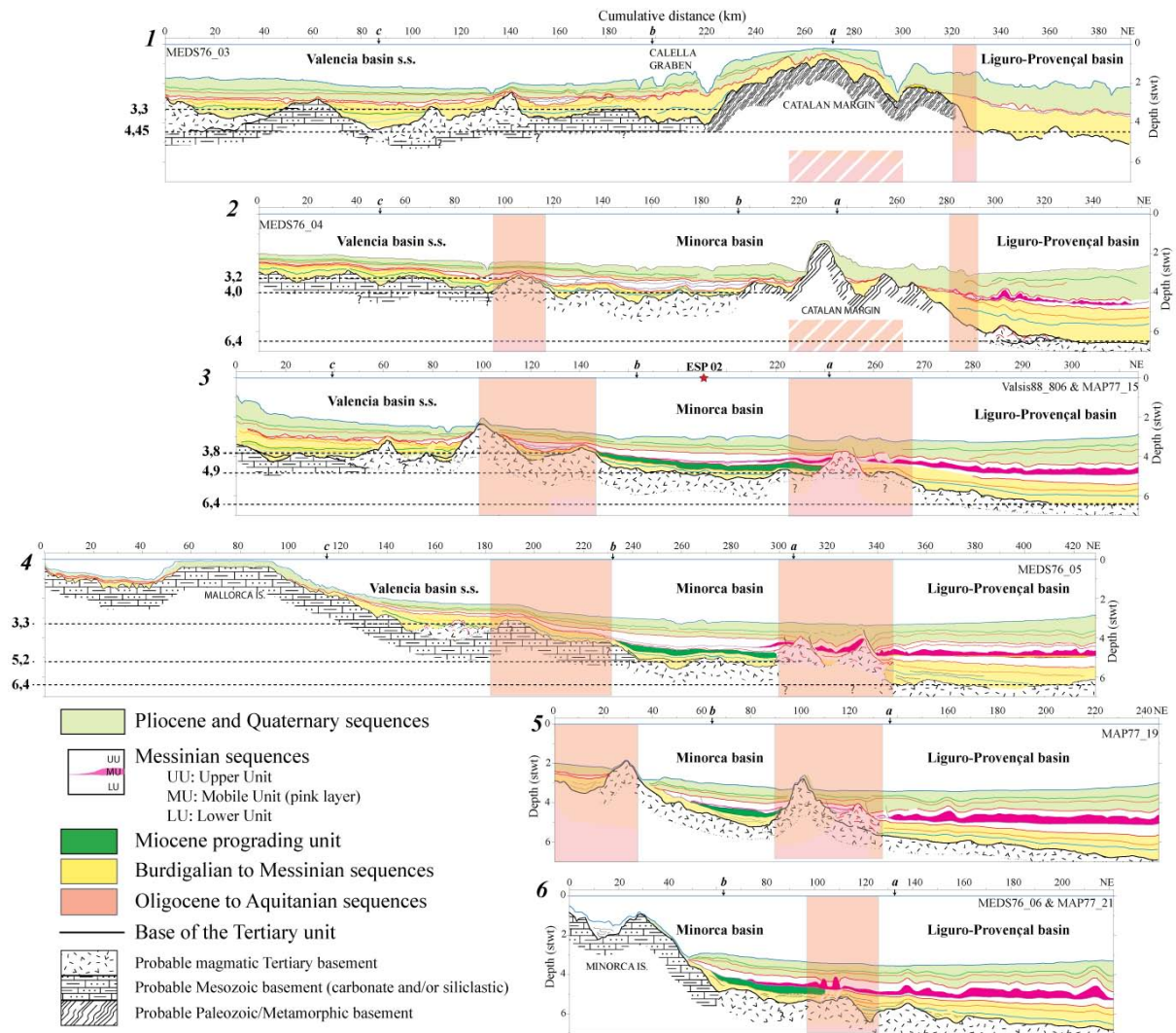


Figure 4A

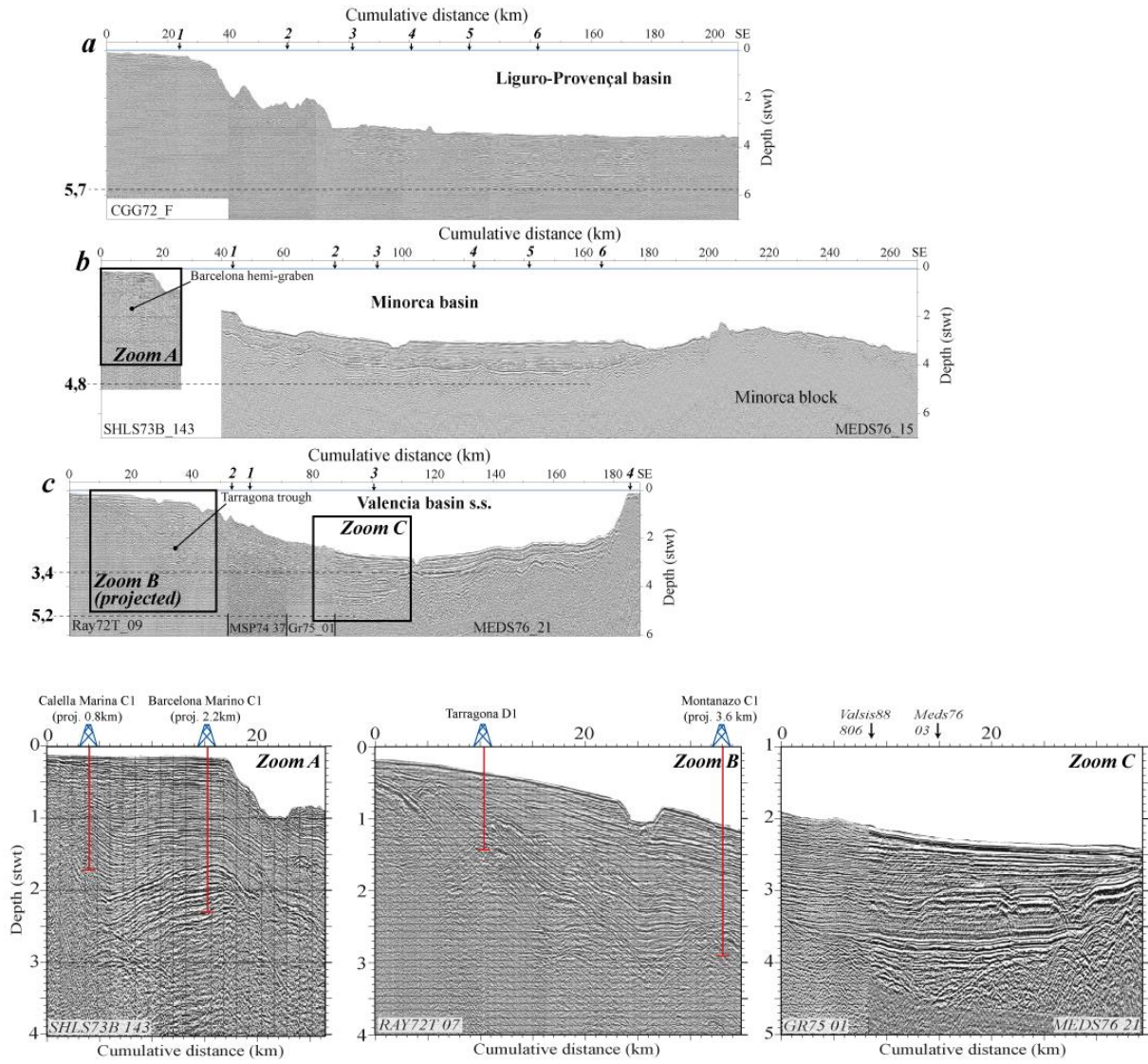
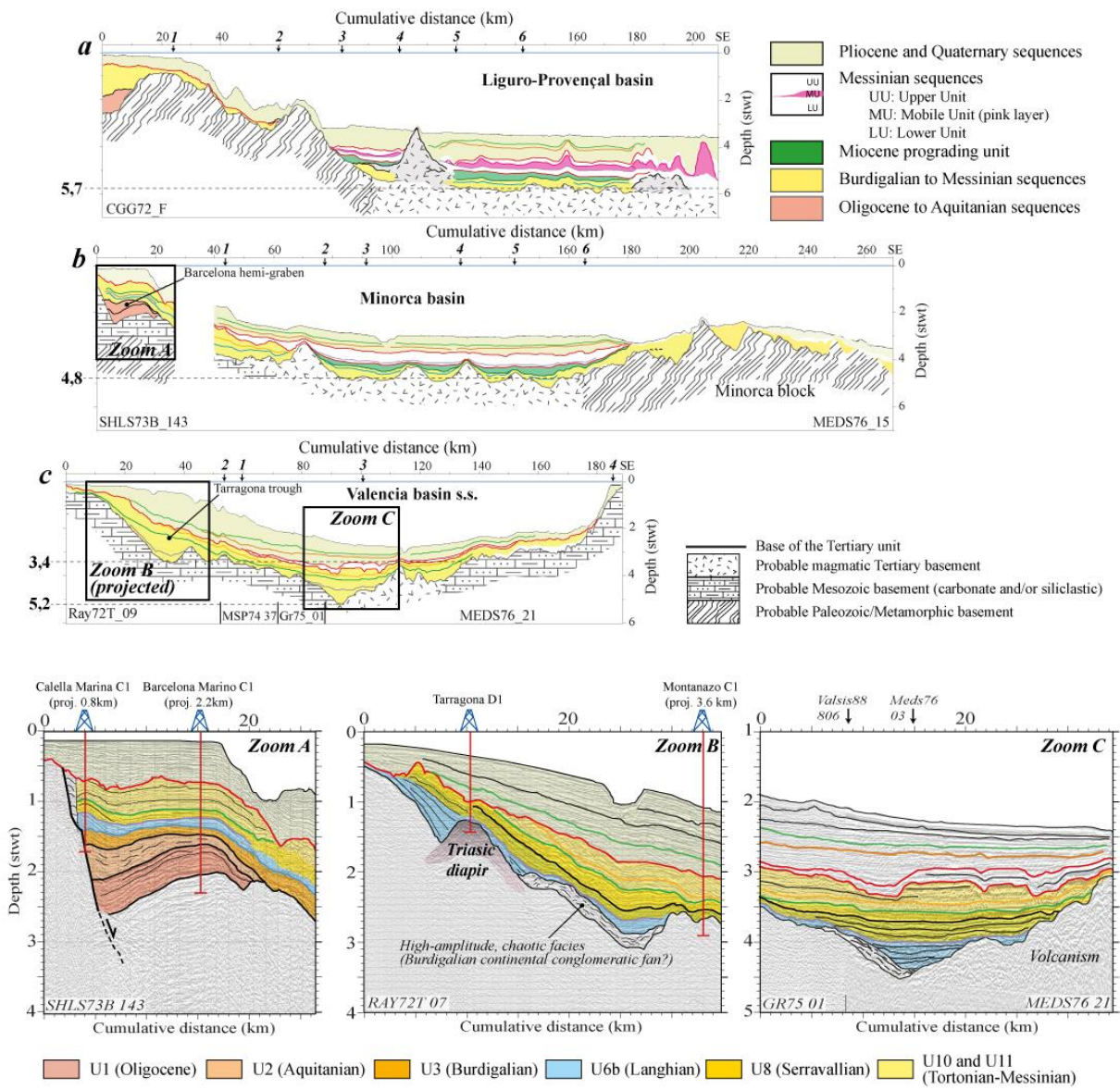
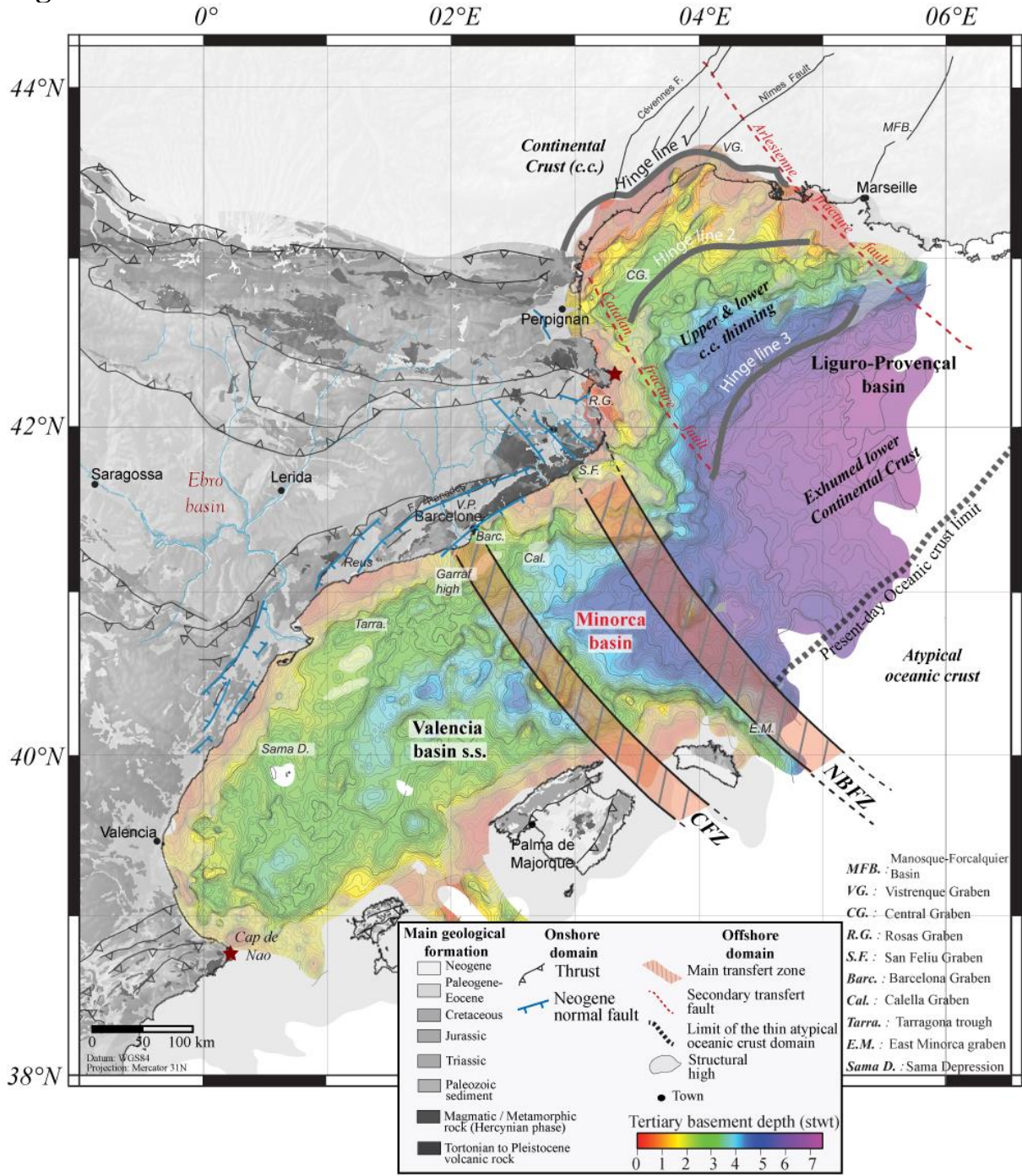


Figure 4B



447 **Figure 5**



448

449

